

Supplementary Material

Two heptanuclear-based 3D metal-organic frameworks with good magnetocaloric effect

Shouying Cao^a, Chenpeng Fan^a, Mengwen Lu^a, Meng Li^a, Yuhang Zhou^a, Hongxia Wang^a, Qingfang Lin^{*b} and Lili Liang^{*a}

^aDepartment of Chemistry, Bengbu Medical College, Bengbu 233030, China.

^bUnited Laboratory for Future International Cooperation, Jilin University, China. E-mail: qingfang@jlu.edu.cn, cl12162@163.com

Contents:

1. Materials and Methods.
2. Fig. S1 Coordination modes of Gd^{III} atoms.
3. Fig. S2 The coordination modes of HCOO⁻ and IDA⁻.
4. Fig. S3 The 3D extended structure of compound **1Gd**.
5. Fig. S4 Powder XRD patterns of **1Gd** and **2Dy**.
6. Fig. S5. FT-IR spectra of **1Gd**.
7. Fig. S6. FT-IR spectra of **2Dy**.
8. Fig. S7 TGA curves of **1Gd** under nitrogen.
9. Fig. S8 TGA curves of **2Dy** under nitrogen.
10. Fig S9. Plot of χ_M^{-1} vs T for **1Gd** and **2Dy**.
11. Fig. S10. Representation of out-of-phase (χ'') (a) and in-phase (χ') (b) frequency dependence of the ac susceptibility components for **2Dy** with zero field.
12. Table S1-S2 Selected bond lengths (Å) and bond angles (°) for **1Gd** and **2Dy**.
13. **Table S3**. The CShM (Continuous Shape Measurements) values of Gd^{III} and Dy^{III} atoms with a nona-coordinate mode.
14. **Table S4**. $-\Delta S_m^{\max}$ value for some Gd^{III}-based MOFs under ΔH by the given temperature.

Materials and Methods

All the chemicals needed for synthesis can be purchased from commercial sources and used as received without further purification. Powder X-ray diffraction data were performed on a Bruker D8X diffractometer equipped with monochromatized Cu-K α ($\lambda = 1.5418 \text{ \AA}$) radiation at room temperature in the range of 5-50°. IR spectra were recorded with a NICOLET iS50 FT-IR spectrometer with KBr pellets in the range of 4000 to 500 cm $^{-1}$. Single-crystal XRD data were obtained from a Bruker Apex II CCD with Mo-K α radiation ($\lambda = 0.71073 \text{ \AA}$) at 293K. TG measurement was carried out on a Diamond thermogravimetric analyzer in flowing N $_2$ atmosphere from 27 to 800 °C with a heating rate of 10 °C min $^{-1}$. The direct current magnetic data were measured at temperature between 2 and 300 K, and the magnetisation isothermal measurements were made in fields of between 0 and 7T on MPMS-XL7 SQUID magnetometer. Elemental analyses of C, H and N were performed on a Perkin-Elmer 240C Elemental Analyzer.

Crystal data of **1Gd**: C $_{15}$ H $_{38}$ Cl $_4$ Gd $_7$ N $_3$ O $_{32}$, $M_r=2015.03$, Hexagonal, $P6_3/m$, $a = 12.1692(5)$, $b = 12.1692(5)$, $c = 18.0220(11) \text{ \AA}$, $V = 2311.3(2) \text{ \AA}^3$, $Z = 2$, $\mu = 10.220 \text{ mm}^{-1}$, $\rho = 2.895 \text{ g.cm}^{-3}$, $F(000) = 1842.0$, $\theta_{\max} = 27.442^\circ$. 18930 measured reflections, 1829 independent reflections. Based on these and 129 parameters, $R_1=0.0145$ ($I>2\sigma(I)$), $wR_2=0.0746$ (all data) were obtained. GOF = 1.075. Crystal size (mm): 0.12 \times 0.09 \times 0.08.

Crystal data of **2Dy**: C $_{15}$ H $_{38}$ Cl $_4$ Dy $_7$ N $_3$ O $_{32}$, $M_r=2051.74$, Hexagonal, $P6_3/m$, $a = 12.0761(3)$, $b = 12.0761(3)$, $c = 17.8609(5) \text{ \AA}$, $V = 2255.73(13) \text{ \AA}^3$, $Z = 2$, $\mu = 11.775 \text{ mm}^{-1}$, $\rho = 3.016 \text{ g.cm}^{-3}$, $F(000)= 1864.0$, $\theta_{\max} = 26.495^\circ$. 18339 measured reflections, 1592 independent reflections. Based on these and 125 parameters, $R_1= 0.0427$ ($I>2\sigma(I)$), $wR_2= 0.0889$ (all data) were obtained. GOF = 1.134. Crystal size (mm): 0.1 x 0.1 x 0.1. CCDC 2203903 and 2203904 contain the supplementary crystallographic data for this paper. These data can be obtained free of charge from the Cambridge Crystallographic Data Centre.

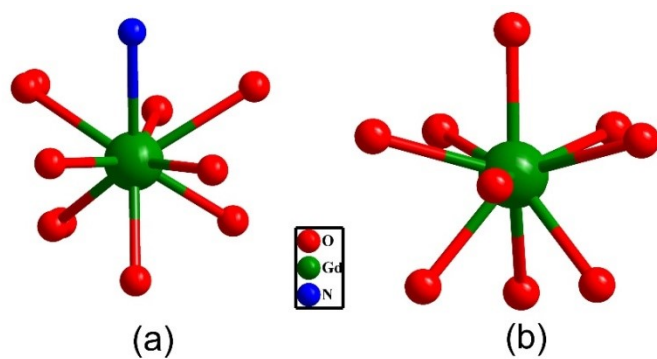


Figure S1. Two coordination modes of Gd^{III} atoms.

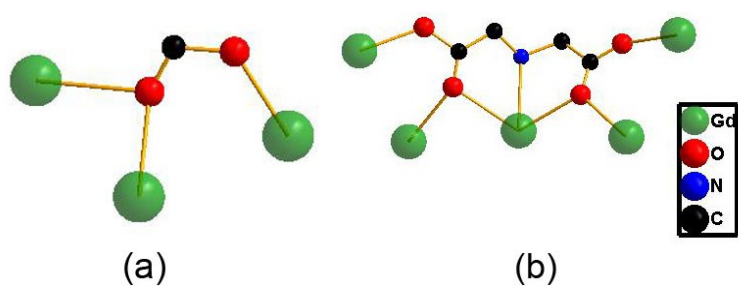


Figure S2. The coordination modes of HCOO⁻ (a) and IDA⁻ (b).

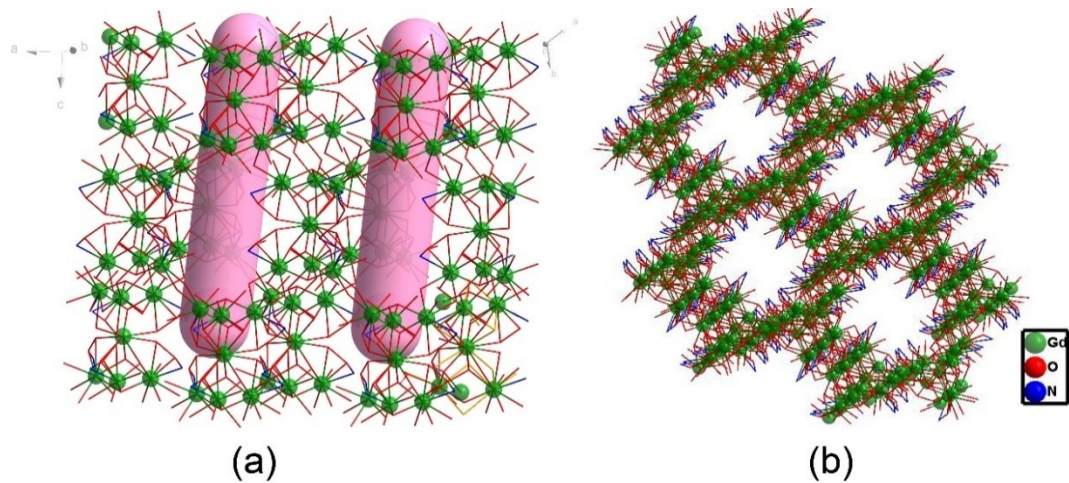


Figure S3. The 3D extended structure of compound 1Gd viewing the *b* (a) and *c* (b) axis.

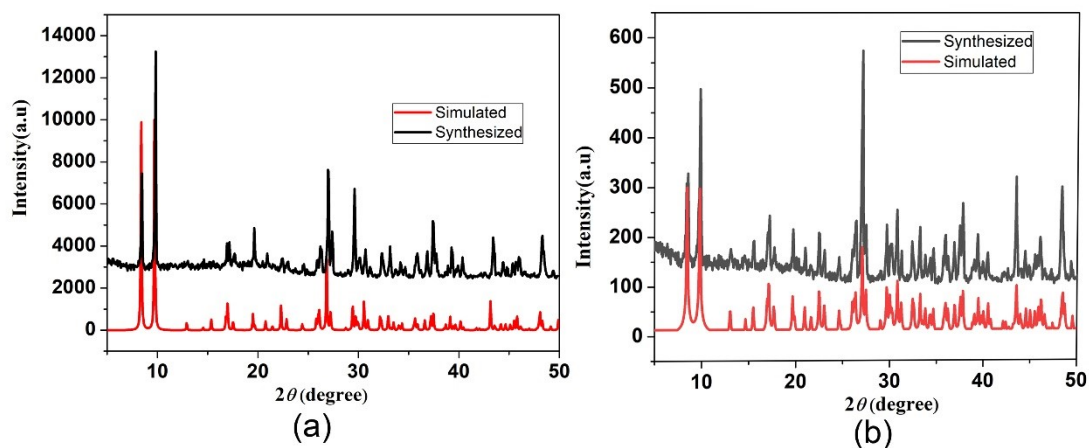


Fig. S4. PXRD patterns of **1Gd** (a) and **2Dy** (b).

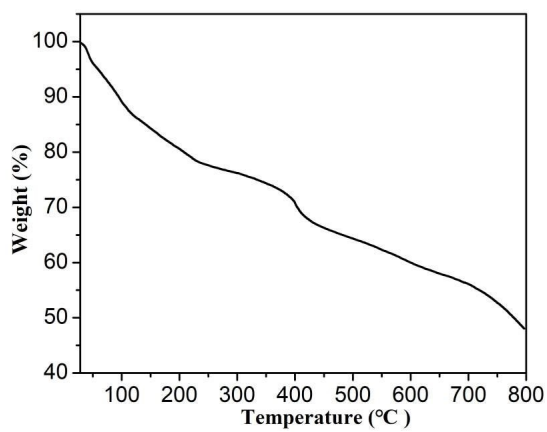


Fig. S5. TG curve of **1Gd**.

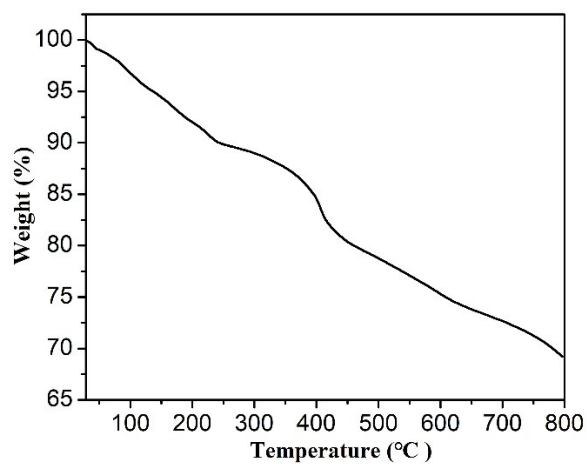


Fig. S6. TG curve of **2Dy**.

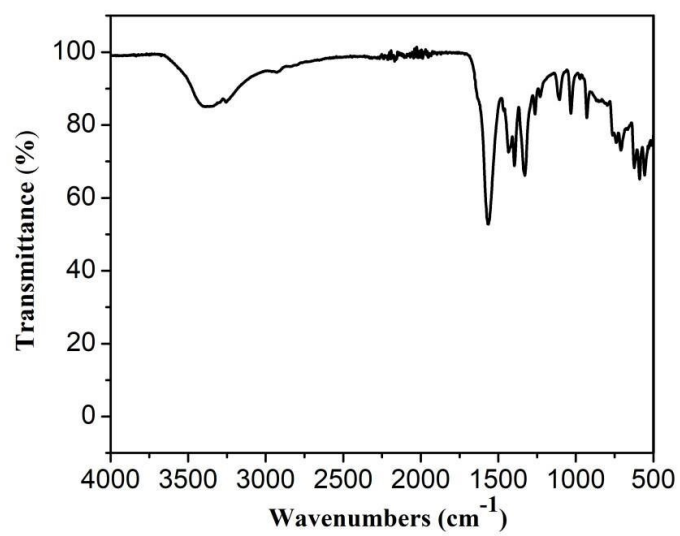


Fig. S7. FT-IR spectra of **1Gd**.

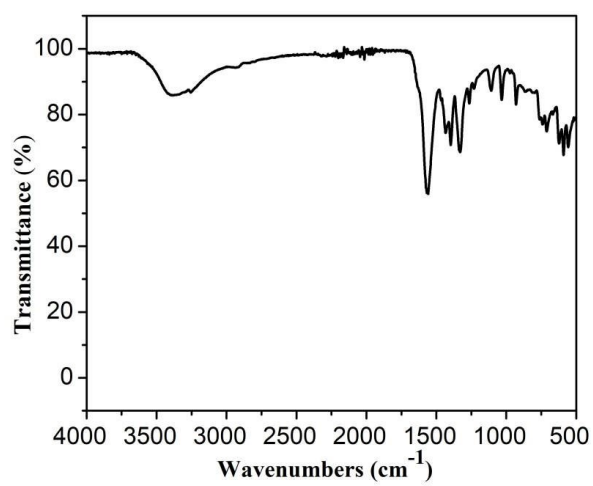


Fig. S8. FT-IR spectra of **2Dy**.

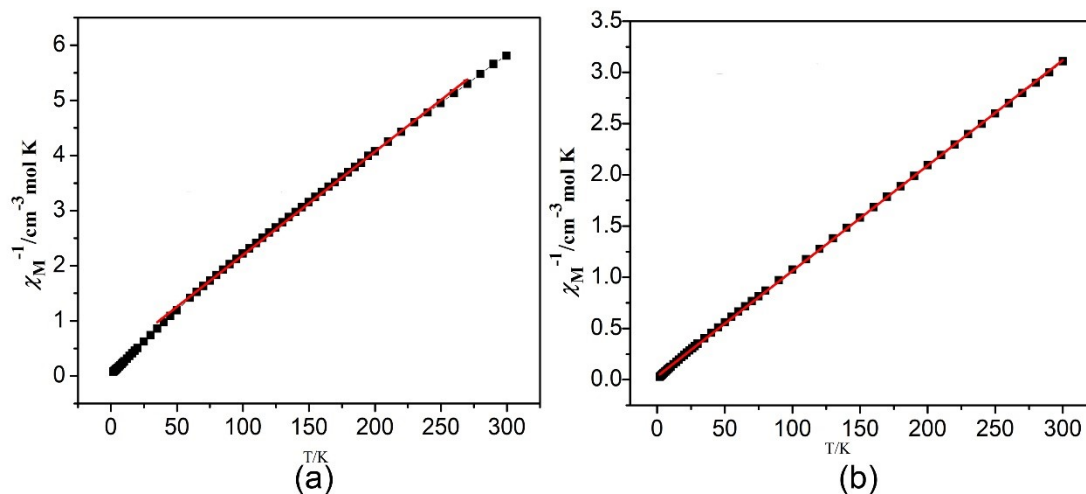


Fig. S9. (a) Plot of χ_M^{-1} vs T for **1Gd**, fit from 270 – 35 K, $c = 53.33 \text{ cm}^3 \text{ K mol}^{-1}$, $\theta = -16.95 \text{ K}$; (b) Plot of χ_M^{-1} vs T for **2Dy**, fit from 300 – 2 K, $c = 97.18 \text{ cm}^3 \text{ K mol}^{-1}$, $\theta = -3.10 \text{ K}$.

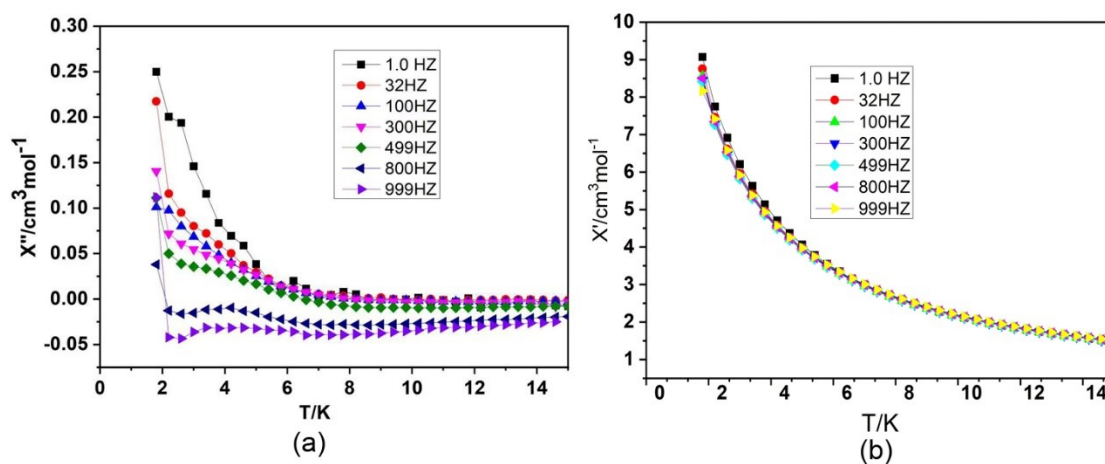


Fig. S10. Representation of weak out-of-phase (χ'') (a) and in-phase (χ') (b) frequency dependence of the ac susceptibility components for **2Dy** with zero field.

Table S1 Selected bond distances (Å) and bond angles (°) for **1 Gd**

1 Gd			
Gd2-O4	2.660(9)	O1-Gd2-O4	111.9(2)
Gd2-O5	2.417(3)	O1-Gd2-N1	66.0(3)
Gd2-O6	2.318(5)	O5-Gd2-O1	129.1(2)
Gd2-O6 ⁵	2.391(5)	O5-Gd2-O4	118.7(3)
Gd2-O7	2.479(6)	O5-Gd2-O7	133.42(15)
Gd1-O4	2.542(10)	O5-Gd2-N1	136.1(3)
Gd1-O6 ⁴	2.401(5)	O6 ⁵ -Gd2-O1	139.00(17)
Gd1-O6 ¹	2.401(5)	O6-Gd2-O1	143.12(17)
Gd1-O6 ³	2.401(5)	O6 ⁵ -Gd2-O4	60.9(2)
Gd1-O65	2.401(5)	O6-Gd2-O4	64.3(2)
Gd1-O6 ²	2.401(5)	O6-Gd2-O5	70.05(19)
Gd1-O6	2.401(5)	O6 ⁵ -Gd2-O5	68.88(19)
Gd2-N1	2.600(12)	Gd2-O6-Gd22	110.27(19)

Symmetry transformations used to generate equivalent atoms:

¹+Y-X,1-X,3/2-Z; ²+Y-X,1-X,+Z; ³+X,+Y,3/2-Z; ⁴1-Y,1+X-Y,3/2-Z; ⁵1-Y,1+X-Y,+Z

Table S2 Selected bond distances (Å) for and bond angles (°) **2 Dy**.

2 Dy			
Dy1-O1	2.399(4)	O1-Dy1-O3 ²	77.4(2)
Dy1-O1W	2.443(6)	O1-Dy1-O3	128.6(3)
Dy1-O2	2.288(6)	O1-Dy1-O5	118.9(3)
Dy1-O2 ²	2.361(6)	O1-Dy1-N1	136.2(3)
Dy1-O3 ³	2.444(6)	O1-Dy1-O3A	128.6(3)
Dy1-O3	2.496(6)	O1W-Dy1-O3	69.8(2)
Dy1-O4 ⁴	2.335(7)	O1W-Dy1-O3 ²	74.4(2)
Dy1-O5	2.635(10)	O1W-Dy1-O5	68.7(3)
Dy1-N1	2.606(16)	O1W-Dy1-N1	88.7(4)
Dy1-O3A	2.496(6)	O1W-Dy1-O3A	69.8(2)
Dy2-O2 ¹	2.379(6)	O2 ³ -Dy1-O1	69.1(2)
Dy2-O2 ⁵	2.379(6)	O2-Dy1-O2 ³	73.9(3)
Dy2-O2 ⁶	2.379(6)	O2-Dy1-O3 ²	92.4(2)
Dy2-O2 ⁷	2.379(6)	O2 ³ -Dy1-O3A	139.1(2)
Dy2-O5	2.504(11)	O2-Dy1-N1	126.1(3)

Symmetry transformations used to generate equivalent atoms:

¹+Y-X,1-X,+Z;²1-X,1-Y,1-Z;³1-Y,1+X-Y,+Z;⁴+Y,1-X+Y,1-Z; ⁵1-Y,1+X-Y,3/2-Z; ⁶+Y-X,1-X,3/2-Z; ⁷+X,+Y,3/2-Z

Table S3. The CShM (Continuous Shape Measurements) values of Gd^{III} and Dy^{III} atoms with a nona-coordinate mode.

Com. ^b Refocde ^a	1Gd		2Dy	
	Gd1	Gd2	Dy1	Dy2
EP-9	33.370/	35.424	31.397/	37.540
OPY-9	29.118/	21.904	22.512/	21.634
HBPY-9	25.450/	17.888	17.643/	20.017
JTC-9	21.302/	15.720	15.253/	17.009
JCCU-9	19.329/	10.529	11.277/	10.467
CCU-9	17.806/	9.337	9.025/	9.317
JCSAPR-9	12.859/	2.092	12.985/	2.451
CSAPR-9	11.088/	1.201	11.553/	1.601
JTCTPR-9	12.230/	2.196	12.683/	2.378
TCTPR-9	10.298/	1.275	12.308/	0.598
JTDIC-9	20.289/	13.333	11.643/	11.793
HH-9	17.951/	9.993	8.821/	11.510
MFF-9	10.759/	1.774	10.182/	1.787

^a EP-9, Enneagon; OPY-9, Octagonal pyramid; HBPY-9, Heptagonal bipyramid; JTC-9, Johnson triangular cupola J3; JCCU-9, Capped cube J8; CCU-9, Spherical-relaxed capped cube; JCSAPR-9, Capped square antiprism J10; CSAPR-9, Spherical capped square antiprism; JTCTPR-9, Tricapped trigonal prism J51; TCTPR-9, Spherical tricapped trigonal prism; JTDIC-9, Tridiminished icosahedron J63; HH-9, Hula-hoop; MFF-9, Muffin. ^b The lanthanide ion in each asymmetric unit of compounds **1Gd** and **2Dy**.

Table S4. $-\Delta S_m^{\max}$ value for some Gd^{III}-based MOFs under ΔH by the given temperature.

Compounds	$-\Delta S_m^{\max}$ (J kg ⁻¹ K ⁻¹)	ΔH (T)	T (K)	Dimensio nality	Ref
[Ln ₅ (μ ₃ -OH) ₅ (μ ₃ -O)(CO ₃) ₂ (HCO ₂) ₂ (C ₄ O ₄)(H ₂ O) ₂]	64.0	9.0	3.0	3D	[1]
[Gd ₆ (OH) ₈ (suc) ₅ nH ₂ O]·2n(H ₂ O)	42.8	7.0	2.0	3D	[2]
{[Ln ₄ (L) _{3,5} (μ ₃ -OH) ₃ (μ ₄ -O)(H ₂ O) ₂]·H ₂ O}n	42.4	7.0	2.0	3D	[3]
H ₂ L= 2,5-pyrazine dicarboxylic acid					
[Ln ₅ (μ ₃ OH) ₆ (TZI) ₃ (DMA) _{1,5} (H ₂ O) _{9,5}]·(DMA)n	41.3	7.0	2.5	3D	[4]
1Gd	40.85	7.0	3.0	3D	This work
{[Gd(fum)(ox) _{0,5} (H ₂ O) ₂]·2H ₂ O}	37.1	7.0	2.0	3D	[5]
Ln ₃ (adipate) _{4,5} (DMF) ₂	36.4	5.0	2.0	3D	[6]

$(\text{H}_6\text{edte})_{0.5}[\text{Gd}^{\text{III}}(\text{ox})_2(\text{H}_2\text{O})]$	35.9	9.0	2.0	3D	[7]
$[\text{Na}@\text{Ln}_8(\text{EDTA})_6(\text{H}_2\text{O})_{22}] \cdot \text{ClO}_4 \cdot 28\text{H}_2\text{O}\}_n$	32.8	7.0	2.0	3D	[8]
$[\text{Gd}_2(\text{N-BDC})_3(\text{dmf})_4]_n$	29.0	7.0	1.8	3D	[9]
$\{\text{H}_2[\text{Gd}_6(\text{OH})_8(\text{H}_2\text{O})_6(\text{p-BDC-F}_4)_6] \cdot 3(2,2'\text{-bpy}) \cdot 6\text{H}_2\text{O}\}$	28.27	8.0	2.0	3D	[10]

References:

1. S. Biswas, A. K. Mondal and S. Konar, *Inorg. Chem.*, 2016, **55**, 2085.
2. Y.C. Chen, F. S. Guo, Y. Z. Zheng, J. L. Liu, J. D. Leng, R. Tarasenko, M. Orendáč, J. Prokleška, V. Sechovský and M. L. Tong, *Chem. Eur. J.*, 2013, **19**, 13504.
3. T. Q. Lu, L. T. Cheng, X. T. Wang, C. Chen, J. Zheng, D. F. Lu and X. Y. Zheng, *Cryst. Growth Des.*, 2022, **22**, 4917.
4. F. Liu, H. Huang, W. Gao, X. M. Zhang and J. P. Liu, *CrystEngComm*, 2017, **19**, 3660.
5. S. J. Liu, T. F. Zheng, J. Bao, P. P. Dong, J. S. Liao, J. L. Chen, H. R. Wen, J. Xu and X. H. Bu, *New J. Chem.*, 2015, **39**, 6970.
6. P. W. Doheny, S. J. Cassidy and P. J. Saines, *Inorg. Chem.*, 2022, **61**, 4957.
7. M. N. Akhtar, Y. C. Chen, M. A. AlDamen and M. L. Tong, *Dalton Trans.*, 2017, **46**, 116.
8. T. Q. Lu, X. T. Wang, L. T. Cheng, C. Chen, H. Y. Shi, J. Zheng and X. Y. Zheng, *Cryst. Growth Des.*, 2021, **21**, 7065.
9. G. Lorusso, M. A. Palacios, G. S. Nichol, E. K. Brechin, O. Roubeau and M. Evangelisti, *Chem. Commun.*, 2012, **48**, 7592.
10. W. Wei, X. Wang, K. Zhang, C. B. Tian and S. W. Du, *Cryst. Growth Des.*, 2019, **19**, 55.